

Multi-Qubit Dynamical Quantum Search Algorithm with Dissipation

A. H. Homid^{1,3,*}, M. Abdel-Aty¹ and A.-S. F. Obada²

¹ University of Science and Technology, Zewail City for Science and Technology, Giza, Egypt

² Faculty of Science, Al-Azhar University, Nasr city 11884, Cairo, Egypt

³ Faculty of Science, Al-Azhar University, Assiut 71524, Egypt

Abstract

We invoke an efficient search algorithms as a key challenge in multi-qubit quantum systems. An original algorithm called dynamical quantum search algorithm from which Grover algorithm is obtained at a specified time is presented. This algorithm is distinguished by accuracy in obtaining high probability of finding any marked state in a shorter time than Grover algorithm time. The algorithm performance can be improved with respect to the different values of the controlled phase. A new technique is used to generate the dynamical quantum gates in the presence of dissipation effect that helps in implementing the current algorithm.

1 Introduction

In the early 1996s, Grover search algorithm (GA) has attracted much interest, since it could work in quantum computer. The quantum search, from computational point of view, is proved to get approximately $O(\sqrt{N})$ operations (in comparison with the $O(N)$ classical operations), which indicates a quadratic speedup [1, 2]. Many efforts have been devoted to achievement of this algorithm theoretically and experimentally by using superconducting qubits [3], trapped ions [4], atom cavity QED systems [5, 6] and nuclear magnetic resonance [7]. Also, most previous studies for improving the quantum GA were general and do not depend on a physical system. Further, all previous implementations of quantum GA have been developed depending on Grover visualizations, where the control phase parameter for the controlled phase gates or oracle is switched to π or $\frac{\pi}{3}$ [2, 8]. However, an interesting work by Long et al [9] has replaced the Grover's arbitrary phase by $\frac{\pi}{2}$. The combination of strong resonant interactions with tight subwavelength traps gives an excellent opportunity to implement much faster quantum gates. However, there is no way to achieve single site addressability in those systems. Existing proposals circumventing this problem [2, 8] do not consider an arbitrary controlled phase parameter or dissipation effect, as the interaction need not to be restricted by certain values of the phase control.

In this article, we propose to add new factors allowing for significant speedup. By combining a multi-qubit system with dissipation taking into account an arbitrary phase control, we can achieve a fast search in a realistic setting. We assume that the control phase is time-dependent to realize the dynamical quantum controlled phase gates. It is shown that the involved time

*E-mail: ahomid86@gmail.com

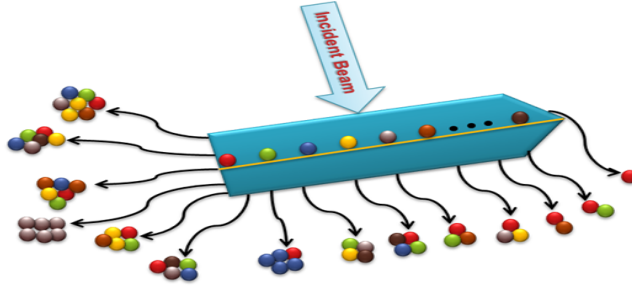


Figure 1: Schematic diagram of quantum dots ensemble. A single surface plasmon injected from outside is coherently scattered by the dots. Our interest is to consider all the possible interactions between any arbitrary pair or more inside the sample. The dissipation effect resulted from the direct contact between the qubits and the plasmons surface.

is the crucial factor for controlling and searching of any marked state regardless the number of qubits. Consequently, we define a new algorithm called a dynamical quantum search algorithm (DQSA). The proposed algorithm is a generalization of Grover algorithm and (i) gives a higher probability of finding any marked state in shorter time, (ii) there is no restriction on the controlled phase parameter and (iii) the presence of qubits dissipation is allowed.

2 Quantum Search Algorithm with Dissipation

The effect of a thermal bath has been used to improve the performance of a quantum adiabatic search algorithm [10]. Vega et al [11] compared the effects of the field dissipation on the algorithm performance with those of a structured environment similar to the one encountered in systems coupled to an electromagnetic field that exists within a photonic crystal. They show that, the algorithm performance has been improved by tuning the environment parameters to certain regimes [12]. We consider the problem with a different perspective, where the algorithm may be implemented within a system taking into account the qubit dissipation. Here, we consider a dense multi-qubit system sample interacting with a single surface plasmon injected from outside. In this case, we consider all the possible interactions between any arbitrary pair or more inside the sample (see Fig.1). The direct contact between the qubits and the plasmons surface yields dissipation effects. As a consequence, we assume that the dipole-dipole interaction potential is nonidentical for all qubits. Other appropriate systems could be superconducting qubits [13, 14] or double quantum dot excitonic systems [15]. Such a model can be written as follows

$$\begin{aligned}
 \hat{H} = & -\lambda \left\{ \sum_{s_1=1}^N J_{s_1} \hat{\sigma}_z^{s_1} + \sum_{s_1, s_2=1}^N J_{s_1 s_2} \hat{\sigma}_z^{s_1} \hat{\sigma}_z^{s_2} + \sum_{s_1, s_2, s_3=1}^N J_{s_1 s_2 s_3} \hat{\sigma}_z^{s_1} \hat{\sigma}_z^{s_2} \hat{\sigma}_z^{s_3} \right. \\
 & \left. + \dots + \sum_{s_1, s_2, s_3, \dots, s_n=1}^N J_{s_1 s_2 s_3 \dots s_n} \hat{\sigma}_z^{s_1} \hat{\sigma}_z^{s_2} \hat{\sigma}_z^{s_3} \dots \hat{\sigma}_z^{s_n} \right\} - i \sum_{v=1}^N \frac{\gamma_v}{2} \hat{\sigma}_+^v \hat{\sigma}_-^v, \quad (1)
 \end{aligned}$$

where $S = \{s_1, s_2, \dots, s_n\}$ refer to the labels of the qubits, N is the number of qubits, γ_u are the dissipation rates of different qubits, J_{s_1}, \dots, J_{s_n} are the energies biases, λ is the coupling constant and $J_{s_1 s_2}, J_{s_1 s_2 s_3}, J_{s_1 s_2 s_3 s_4}, \dots, J_{s_1 \dots s_n}$ are the interaction energies between two qubits or more. In the proposed model, the interaction energy between qubits is set to provide the maximum ferromagnetic coupling. Here, we consider the number of qubits is $N = 9$ and $S = \{s_1, s_2, \dots, s_9\}$. To realize the dynamics of the controlled phase gates for different qubits, we write, for simplicity, that the sub-indexes $s_1 \equiv s, s_2 \equiv j, s_3 \equiv k$ and $s_4 \equiv l, s_5 \equiv m, s_6 \equiv n$ and so on.

First, we use the case of $N = 2$ and $S = \{s_1, s_2\}$. Hence, the time evolution of system (1) in these cases is given by $\hat{U}_2(t)$. Therefore, we can realize a two-qubit dynamical controlled phase gates in the presence of qubits dissipation in the following context.

- If $J_1 = J_2 = \pm(J_{11} + J_{22})$ and $J_{12} = J_{21} = \pm\frac{1}{2}J_1$, we get $\hat{U}_2(t) \rightarrow \hat{P}_{ee}(t; \gamma_1, \gamma_2)$ and $\hat{U}_2(t) \rightarrow \hat{P}_{gg}(t; \gamma_1, \gamma_2)$.
- If $J_1 = \pm(J_{11} + J_{22})$, $J_2 = -J_1$ and $J_{12} = J_{21} = \pm\frac{1}{2}J_2$, we obtain $\hat{U}_2(t) \rightarrow \hat{P}_{eg}(t; \gamma_1, \gamma_2)$ and $\hat{U}_2(t) \rightarrow \hat{P}_{ge}(t; \gamma_1, \gamma_2)$.

Second, we use the case of $N = 3$ and $S = \{s_1, s_2, s_3\}$. In this case, it is assumed that (i) $J_{kkj} = -J_{kjk}$, $J_{jkk} = -\frac{1}{2}J_{jjj}$ and $J_{kj} = J_{jk}$, $\forall j \neq k$; (ii) $F_{sjk} = J_{ss} + J_{jj} + J_{kk}$ and $J_{sjk} = w_1$, $\forall s \neq j \neq k$. Hence, after applying these steps, the time evolution of system (1) is given by $\hat{U}_3(t)$. So, we can realize three-qubit dynamical controlled phase gates in the presence of qubits dissipation as follows.

- If $J_s = \pm F_{sjk}$, $J_{jk} = \pm\frac{1}{2}J_s$ ($\forall s \neq j \neq k$) and $w_1 = \pm\frac{1}{6}F_{sjk}$, we get $\hat{U}_3(t) \rightarrow \hat{P}_{eee}(t; \gamma_1, \gamma_2, \gamma_3)$ and $\hat{U}_3(t) \rightarrow \hat{P}_{ggg}(t; \gamma_1, \gamma_2, \gamma_3)$.
- If $J_1 = J_2 = \pm F_{sjk}$, $J_3 = \mp F_{sjk}$, $J_{12} = \pm\frac{1}{2}J_1$, $J_{13} = J_{23} = \mp\frac{1}{2}J_2$ and $w_1 = \mp\frac{1}{6}F_{sjk}$ we obtain $\hat{U}_3(t) \rightarrow \hat{P}_{eeg}(t; \gamma_1, \gamma_2, \gamma_3)$ and $\hat{U}_3(t) \rightarrow \hat{P}_{gge}(t; \gamma_1, \gamma_2, \gamma_3)$.
- If $J_1 = J_3 = \pm F_{sjk}$, $J_2 = \mp F_{sjk}$, $J_{12} = J_{23} = \pm\frac{1}{2}J_2$, $J_{13} = \pm\frac{1}{2}J_3$ and $w_1 = \mp\frac{1}{6}F_{sjk}$, then $\hat{U}_3(t) \rightarrow \hat{P}_{ege}(t; \gamma_1, \gamma_2, \gamma_3)$ and $\hat{U}_3(t) \rightarrow \hat{P}_{geg}(t; \gamma_1, \gamma_2, \gamma_3)$.
- If $J_1 = \pm F_{sjk}$, $J_2 = J_3 = \mp F_{sjk}$, $J_{12} = J_{13} = \pm\frac{1}{2}J_3$, $J_{23} = \pm\frac{1}{2}J_1$ and $w_1 = \pm\frac{1}{6}F_{sjk}$, one obtains $\hat{U}_3(t) \rightarrow \hat{P}_{egg}(t; \gamma_1, \gamma_2, \gamma_3)$ and $\hat{U}_3(t) \rightarrow \hat{P}_{gee}(t; \gamma_1, \gamma_2, \gamma_3)$.

Third, when $N = 4$ and $S = \{s_1, s_2, s_3, s_4\}$, and assume that (i) $J_{jsks} = -J_{sjks}$ and $J_{sjks} = -J_{jssk}$, $\forall s \neq j \neq k$; (ii) $J_{kss} = -\frac{1}{3}J_{kkk}$, $J_{ssk} = -J_{skk}$ and $J_{skk} = -J_{skks}$, $\forall s \neq k$; (iii) $J_{jjkk} = 0$, $J_{jk} = J_{kj}$ and $J_{ssjk} = -J_{jkss}$, $\forall j \neq k$, the time evolution of system (1) is given by $\hat{U}_4(t)$. After that, we write (i) $E_{sjkl} = (J_{ss} + J_{ssss} + J_{jj} + J_{jjjj} + J_{kk} + J_{kkkk} + J_{ll} + J_{llll})$, $\forall s \neq j \neq k \neq l$; (ii) $w_1 = J_{sjk}(s, j, k = 1, 2, 3)$, $w_2 = J_{sjk}(s, j, k = 1, 2, 4)$, $w_3 = J_{sjk}(s, j, k = 1, 3, 4)$ and $w_4 = J_{sjk}(s, j, k = 2, 3, 4)$, $\forall s \neq j \neq k$; (iii) $\frac{1}{6}E_{sjk4} = a_1$, $\frac{1}{6}E_{sjk3} = a_2$, $\frac{1}{6}E_{sjk2} = a_3$ and $\frac{1}{6}E_{sjk1} = a_4$. Now, one can realize the four-qubit dynamical controlled phase gates in following.

- If $J_{sjkl} = \frac{1}{24}E_{sjkl}$, $J_s = \pm E_{sjkl}$, $J_{jk} = \pm\frac{1}{2}J_s$ ($\forall s \neq j \neq k$), $w_1 = \pm a_1$, $w_2 = \pm a_2$, $w_3 = \pm a_3$ and $w_4 = \pm a_4$, one obtains $\hat{U}_4(t) \rightarrow \hat{P}_{eeee}(t; \gamma_1, \dots, \gamma_4)$ and $\hat{U}_4(t) \rightarrow \hat{P}_{gggg}(t; \gamma_1, \dots, \gamma_4)$.
- If $J_{sjkl} = -\frac{1}{24}E_{sjkl}$, $J_1 = J_2 = J_3 = \pm E_{sjkl}$, $J_4 = \mp E_{sjkl}$, $J_{12} = J_{13} = J_{23} = \pm\frac{1}{2}J_2$, $J_{14} = J_{24} = J_{34} = \mp\frac{1}{2}J_3$, $w_1 = \pm a_1$, $w_2 = \mp a_2$, $w_3 = \mp a_3$ and $w_4 = \mp a_4$, then $\hat{U}_4(t) \rightarrow \hat{P}_{eegg}(t; \gamma_1, \dots, \gamma_4)$ and $\hat{U}_4(t) \rightarrow \hat{P}_{ggge}(t; \gamma_1, \dots, \gamma_4)$.

- If $J_{sjkl} = -\frac{1}{24}E_{sjkl}$, $J_1 = J_2 = J_4 = \pm E_{sjkl}$, $J_3 = \mp E_{sjkl}$, $J_{12} = J_{14} = J_{24} = \mp \frac{1}{2}J_3$, $J_{13} = J_{23} = J_{34} = \pm \frac{1}{2}J_3$, $w_1 = \mp a_1$, $w_2 = \pm a_2$, $w_3 = \mp a_3$ and $w_4 = \mp a_4$, obtain $\hat{U}_4(t) \rightarrow \hat{P}_{eege}(t; \gamma_1, \dots, \gamma_4)$ and $\hat{U}_4(t) \rightarrow \hat{P}_{ggeg}(t; \gamma_1, \dots, \gamma_4)$.
- If $J_{sjkl} = \frac{1}{24}E_{sjkl}$, $J_1 = J_2 = \pm E_{sjkl}$, $J_3 = J_4 = \mp E_{sjkl}$, $J_{12} = J_{34} = \pm \frac{1}{2}J_1$, $J_{13} = J_{14} = J_{23} = J_{24} = \pm \frac{1}{2}J_4$, $w_1 = \mp a_1$, $w_2 = \mp a_2$, $w_3 = \pm a_3$ and $w_4 = \pm a_4$, then $\hat{U}_4(t) \rightarrow \hat{P}_{eeeg}(t; \gamma_1, \dots, \gamma_4)$ and $\hat{U}_4(t) \rightarrow \hat{P}_{ggee}(t; \gamma_1, \dots, \gamma_4)$.
- If $J_{sjkl} = -\frac{1}{24}E_{sjkl}$, $J_1 = J_3 = J_4 = \pm E_{sjkl}$, $J_2 = \mp E_{sjkl}$, $J_{12} = J_{23} = J_{24} = \mp \frac{1}{2}J_4$, $J_{13} = J_{14} = J_{34} = \pm \frac{1}{2}J_1$, $w_1 = \mp a_1$, $w_2 = \mp a_2$, $w_3 = \pm a_3$ and $w_4 = \mp a_4$, one obtains $\hat{U}_4(t) \rightarrow \hat{P}_{egee}(t; \gamma_1, \dots, \gamma_4)$ and $\hat{U}_4(t) \rightarrow \hat{P}_{geeg}(t; \gamma_1, \dots, \gamma_4)$.
- If $J_{sjkl} = \frac{1}{24}E_{sjkl}$, $J_1 = J_3 = \pm E_{sjkl}$, $J_2 = J_4 = \mp E_{sjkl}$, $J_{12} = J_{14} = J_{23} = J_{34} = \pm \frac{1}{2}J_4$, $J_{13} = J_{24} = \mp \frac{1}{2}J_4$, $w_1 = \mp a_1$, $w_2 = \pm a_2$, $w_3 = \mp a_3$ and $w_4 = \pm a_4$, we get $\hat{U}_4(t) \rightarrow \hat{P}_{egeg}(t; \gamma_1, \dots, \gamma_4)$ and $\hat{U}_4(t) \rightarrow \hat{P}_{gege}(t; \gamma_1, \dots, \gamma_4)$.
- If $J_{sjkl} = \frac{1}{24}E_{sjkl}$, $J_1 = J_4 = \pm E_{sjkl}$, $J_2 = J_3 = \mp E_{sjkl}$, $J_{12} = J_{13} = J_{24} = J_{34} = \pm \frac{1}{2}J_2$, $J_{14} = J_{23} = \pm \frac{1}{2}J_4$, $w_1 = \pm a_1$, $w_2 = \mp a_2$, $w_3 = \mp a_3$ and $w_4 = \pm a_4$, then $\hat{U}_4(t) \rightarrow \hat{P}_{egge}(t; \gamma_1, \dots, \gamma_4)$ and $\hat{U}_4(t) \rightarrow \hat{P}_{geeg}(t; \gamma_1, \dots, \gamma_4)$.
- If $J_{sjkl} = -\frac{1}{24}E_{sjkl}$, $J_1 = \pm E_{sjkl}$, $J_2 = J_3 = J_4 = \mp E_{sjkl}$, $J_{12} = J_{13} = J_{14} = \mp \frac{1}{2}J_1$, $J_{23} = J_{24} = J_{34} = \mp \frac{1}{2}J_2$, $w_1 = \pm a_1$, $w_2 = \pm a_2$, $w_3 = \pm a_3$ and $w_4 = \mp a_4$, one obtains $\hat{U}_4(t) \rightarrow \hat{P}_{eggg}(t; \gamma_1, \dots, \gamma_4)$ and $\hat{U}_4(t) \rightarrow \hat{P}_{geee}(t; \gamma_1, \dots, \gamma_4)$.

In the above notations (First, Second and Third) the top sign is used to realize the first part while the lower sign is used to realize the second part.

Using the same technique, one realizes the dynamical controlled phase gates in the presence of the dissipation for the case of $N = 5, 6, 7, 8$ and 9 . The calculations of the dynamics gates when $N = 5, 6, 7, 8$ and 9 lengthy and are not presented here. But we present some results of application of these dynamic controlled phase gates for different qubits in calculating the probabilities of marked and un-marked states in the presence of dissipation, see appendix. If $\gamma_i = 0, i = 1, 2, \dots, 9$, one obtains the ideal dynamical controlled phase gates. The dynamical conditional phase gates for N qubits is governed by a dynamical control parameter phase

$$\beta_N(t) = \frac{2^N \theta_N}{\hbar} \lambda t. \quad (2)$$

The parameter θ_N for different qubits is given by:

$$\begin{aligned} \theta_2 &= \sum_{r=1}^2 J_{rr}, \theta_3 = \theta_2 + J_{33}, \theta_4 = \sum_{r=1}^4 (J_{rr} + J_{rrrr}), \\ \theta_5 &= \theta_4 + J_{55}, \theta_6 = \sum_{r=1}^6 (J_{rr} + J_{rrrr} + J_{rrrrrr}), \theta_7 = \theta_6 + J_{77}, \\ \theta_8 &= \sum_{r=1}^8 (J_{rr} + J_{rrrr} + J_{rrrrrr} + J_{rrrrrrrr}) \text{ and } \theta_9 = \theta_8 + J_{99}. \end{aligned}$$

For an individual qubit and based on the available experimental data as given in [16,17], we assume that the value of $\lambda J_s = \theta_N$ ($s = 1, 2, 3, \dots, N$) to realize one qubit gate in the presence of dissipation. Now, one can realize a one-qubit gate $\hat{W}(\gamma_s)$ in the following context. The time evolution of system under $\hat{H}_s = -\lambda J_s \hat{\sigma}_z^s$ is given by $\hat{V}_1^s(t)$, and the time evolution of system under $\hat{H}^s = \exp(i\pi \hat{\sigma}_y^s/4) \hat{H}_s \exp(-i\pi \hat{\sigma}_y^s/4) - \frac{i\gamma_s}{2} \hat{\sigma}_+^s \hat{\sigma}_-^s$, is given by $\hat{V}_2^s(t)$. Then, it is concluded that

$$\begin{aligned} \hat{W}(\gamma_s) &= e^{\frac{i\pi}{2} \hat{V}_1^s} \left(\frac{\pi \hbar}{4\theta_N} \right) \hat{V}_2^s \left(\frac{\pi \hbar}{4\xi_s} \right) \hat{V}_1^s \left(\frac{\pi \hbar}{4\theta_N} \right) = \frac{1}{\sqrt{2}} \exp\left(\frac{-\pi \gamma_s}{16\xi_s}\right) \left\{ \left(1 + \frac{\gamma_s}{4\xi_s}\right) |g_s\rangle \langle g_s| \right. \\ &\quad \left. + \frac{\theta_N}{\xi_s} |g_s\rangle \langle e_s| + \frac{\theta_N}{\xi_s} |e_s\rangle \langle g_s| - \left(1 - \frac{\gamma_s}{4\xi_s}\right) |e_s\rangle \langle e_s| \right\}, \end{aligned} \quad (3)$$

with $4\xi_s = \sqrt{16\theta_N^2 - \gamma_s^2}$.

The current algorithm has two registers, the N qubits in the first register and one qubit in the second register. Therefore, the proposed system contains $N+1$ qubits. Initialize an $N+1$ qubits system to the state $|g_1, g_2, \dots, g_N\rangle |e_{N+1}\rangle$, where the state in the second register refers to the excited state of an auxiliary working qubit. Now, we implement the dynamical quantum search algorithm in the presence of dissipation as follows: Performing $\hat{W}^{\otimes N}(\gamma_1, \gamma_2, \dots, \gamma_N)$ on the first register and performing $\hat{W}(\gamma_{N+1})$ on the second register. Then, we apply the dynamical controlled phase gates $\hat{P}_x(t; \gamma_1, \dots, \gamma_N)$ on the first register (where $x \in \Lambda$ and $\Lambda = \{g_1g_2\dots g_{N-1}g_N, g_1g_2\dots g_{N-1}e_N, g_1g_2\dots g_{N-2}e_{N-1}g_N, \dots, e_1e_2\dots e_{N-1}g_N, e_1e_2\dots e_{N-1}e_N\}$) and apply $\hat{W}^{-1}(\gamma_{N+1})$ on the second register. Consequently, it is to observe the state of Λ which has been stored in the data qubits before applying the dynamical controlled phase gates or oracles. Also, we note that after applying this step the dynamical controlled phase gates have effects only on the states to be searched in the first register and the state of the second register does not change. So, we can omit the auxiliary working qubit or one can discard the state of the second register at this point via normalization of this state. Finally, we apply a new dynamical diffusion transform matrix, $\hat{D}(t; \gamma_1, \dots, \gamma_N) = \exp(i\beta_N(t))\hat{W}^{\otimes N}(\gamma_1, \dots, \gamma_N)\hat{P}_{g_1g_2\dots g_N}(t; \gamma_1, \dots, \gamma_N)\hat{W}^{\otimes N}(\gamma_1, \dots, \gamma_N)$, on the first register and measure the resulting state. Consequently, the final formula of the dissipation DQSA is given by:

$$\text{DQSA} = \prod_{i=1}^{N-1} \left\{ \hat{D}(t; \gamma_1, \dots, \gamma_N) \hat{P}_x(t; \gamma_1, \dots, \gamma_N) \right\}^{N-i} \hat{W}^{\otimes N}(\gamma_1, \dots, \gamma_N) |g_1g_2\dots g_{N-1}g_N\rangle, \quad (4)$$

where $N-1$ is the number of iterations. In the absence of dissipation, the matrix elements of \hat{D} , at any time, are $D_{ij} = D_{ji}$ for $i \neq j$ ($i, j = 1, 2, \dots, 2^N$) while all diagonal elements D_{ii} are equal. Also, in the presence of qubits dissipation rates, whether similar or different values, the matrix elements at any time are $D_{ij} = D_{ji}$ for $i \neq j$ while all diagonal elements D_{ii} are often close to each others.

Now, we give the probabilities definitions of finding any marked state $\rho_{r_1r_2\dots r_N}$ and finding unmarked states (or remaining states) $\varrho_{j_1j_2\dots j_N}$. The probabilities are exactly calculated in the presence of different values of dissipation rates and different N , where both of $r_1r_2\dots r_N$ and $j_1j_2\dots j_N$ are one subset of the set Λ . The probabilities $\rho_{r_1r_2\dots r_N}$ and $\varrho_{j_1j_2\dots j_N}$ are give by:

$$\rho_{r_1r_2\dots r_N} = \rho_{r_1r_2\dots r_N}(t; \gamma_1, \dots, \gamma_N) = \left| \langle r_1r_2\dots r_N | I_{N-1}(t; \gamma_1, \dots, \gamma_N) \hat{W}^{\otimes N}(\gamma_1, \dots, \gamma_N) | g_1g_2\dots g_N \rangle \right|^2. \quad (5)$$

$$\varrho_{j_1j_2\dots j_N} = \varrho_{j_1j_2\dots j_N}(t; \gamma_1, \dots, \gamma_N) = \left| \langle j_1j_2\dots j_N | I_{N-1}(t; \gamma_1, \dots, \gamma_N) \hat{W}^{\otimes N}(\gamma_1, \dots, \gamma_N) | g_1g_2\dots g_N \rangle \right|^2, \quad (6)$$

where $I_{N-1}(t; \gamma_1, \dots, \gamma_N) = \prod_{i=1}^{N-1} \left\{ \hat{D}(t; \gamma_1, \dots, \gamma_N) \hat{P}_{r_1r_2\dots r_N}(t; \gamma_1, \dots, \gamma_N) \right\}^{N-i}$. From Eq.6, in calculating the probabilities of unmarked states, it should be noted that at least one of $j_1j_2\dots j_N$ is not equal to one of $r_1r_2\dots r_N$ for the same qubit. Here, we write, for simplicity, that the sub-indexes in the marked state $\rho_{e_1e_2} \equiv \rho_{ee}$ and un-marked states ($\varrho_{e_1g_2}, \varrho_{g_1e_2}, \varrho_{g_1g_2} \equiv \text{Pr. r. s.}$); marked state $\rho_{e_1g_2e_3} \equiv \rho_{ege}$ and unmarked states ($\varrho_{e_1e_2e_3}, \varrho_{e_1e_2g_3}, \varrho_{e_1g_2g_3}, \varrho_{g_1e_2e_3}, \varrho_{g_1e_2g_3}, \varrho_{g_1g_2e_3}, \varrho_{g_1g_2g_3} \equiv \text{Pr. r. s.}$); and so on for all states of the N -qubit. Also, $\rho_{g_1e_2g_3e_4} \equiv \rho_{gege}$ and so on.

3 Discussion

In table (1), we compare our proposed algorithm (OA) results with Grover algorithm's results. It is shown that the probability reach 100% for the two-qubit case, in both: our case and GA case,

No.	$\lambda t_p/\hbar$	Present Pr.	$\lambda t_G/\hbar$	Grover Pr.
2	$(0.9425\pi)/4\theta_2$	1	$\pi/4\theta_2$	1
3	$(0.6723\pi)/8\theta_3$	1	$\pi/8\theta_3$	0.9453
4	$(0.6933\pi)/16\theta_4$	1	$\pi/16\theta_4$	0.9613
5	$(0.8661\pi)/32\theta_5$	1	$\pi/32\theta_5$	0.9992
6	$(0.9899\pi)/64\theta_6$	0.9635	$\pi/64\theta_6$	0.9635
7	$(0.9906\pi)/128\theta_7$	0.8335	$\pi/128\theta_7$	0.8335
8	$(0.9906\pi)/256\theta_8$	0.6503	$\pi/256\theta_8$	0.6503
9	$(0.995\pi)/512\theta_9$	0.4662	$\pi/512\theta_9$	0.4662

Table 1: A comparison of the time (t_p) of the present algorithm and Grover time (t_G) for finding higher probability (Pr.) of any marked state of different qubits in the case of $\gamma_i = 0$, $i = 1, 2, \dots, 9$.

but the time needed in our case, t_p , is shorter than the Grover time, t_G , (say, $t_p = 0.9425\pi\hbar/4\lambda\theta_2$ and $t_G = \pi\hbar/4\lambda\theta_2$). This means that the efficiency of our algorithm is higher than the efficiency of GA. Once we increase the number of involved qubits, we see that a significant difference between OA and GA, is seen. The probability of finding any marked state using 3 qubits, 4 qubits and 5 qubits in OA is 100% while the corresponding case using GA does not exceed 94.53% for 3 qubits, 96.13% for 4 qubits and 99.92% for 5 qubits. Moreover, the times needed of finding any marked state are shorter than Grover times. This is an interesting advantage of the proposed algorithm since the sensitivity is much higher than the Grover sensitivity to the number of qubits. Also, we can say that using OA, exact observation is clearly obtained even whether the number of involved qubits gets higher (say 5) and one still have 100% probability of finding any marked states. When we consider the number of qubits is greater than or equal 6, it is shown that the same probability of finding any marked state is obtained using OA and GA, but the time needed to obtain such probability is shorter in our case, which is still gives OA an advantage. It is interesting to observe here that as the number of qubits is increased the probability find any desired state still coincide using OA while in Grover case there does not coincide, where from 1 – 6 qubits the results do not coincide with the fact that increasing the number of qubits leads to decreasing the probability. Moreover, as the number is increased further, GA shows the logic behavior. In these calculations, we expect that our results (times and probabilities) are almost the same as GA for the large number of qubits (say, $N > 12$). The reason of such agreement between our results and Grover results is that when N is increased the time for finding the highest probability of any marked state is increased to reach almost $\frac{\pi\hbar}{2^{13}\lambda\theta_{13}}$ for finding the probability of any marked state when $N = 13$. After that, one obtains the highest probability for finding any desired states for the different qubits at times $\frac{\pi\hbar}{2^r\lambda\theta_r}$ ($r = 13, 14, \dots, N$), this case is compatible with Grover case. This observation shows that using the dynamical quantum search algorithm has some advantage, where GA is obtained as a special case from the proposed general algorithm.

In Fig.2 we plot the probabilities of finding any marked or unmarked states as a function of dynamical phase $\beta_N(t)/\pi$, $N = 2, 3, \dots, 9$, in the absence of dissipation. It is shown that for 2, 3, 4 and 5 qubits, see Fig.2a and Fig.2b, the probabilities of marked states reach one at several points rather than Grover observation, where GA shows the maximum probability at $\beta_N(t) = \pi$ only. In 3 qubits and 4 qubits cases, we find that the behavior of curves peaks are between the two maxima there is a local minimum. While 2 and 5 qubits cases the maximum stays longer as a function of the phase, which means that the long lived maximum probability is obtained for 2 and 5 qubits compared with 3 and 4 qubits cases where the maximum stays for a short period. This observation is no longer existing once the number of qubits is increased (say ≥ 6), where the maxima probability always less than one, see Fig.2c and Fig.2d. Also, the

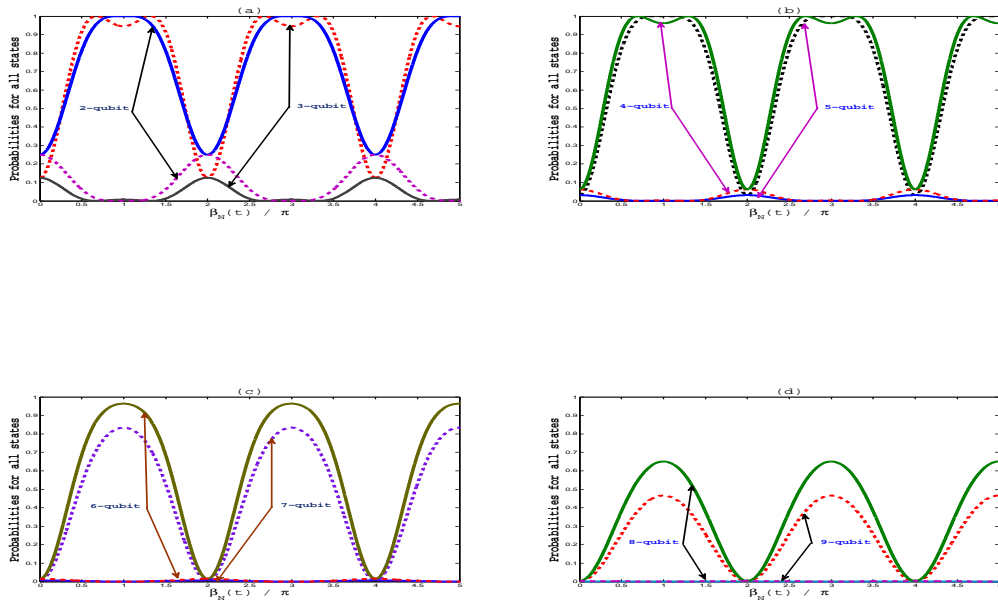


Figure 2: Dynamical quantum search algorithm for the multi qubits in the absence of dissipation for all marked states (solid lines for 2-, 4-, 6- and 8-qubit; dashed lines for 3-, 5-, 7- and 9-qubit) and all un-marked states (dashed lines for 2-, 4-, 6- and 8-qubit; solid lines for 3-, 5-, 7- and 9-qubit), where $N = 2, 3$ in (a), $N = 4, 5$ in (b), $N = 6, 7$ in (c) and $N = 8, 9$ in (d).

unmarked states are observed for the low number of qubits and reach the maximum of 25% for 2 qubits case, while this value is decreased once the number of qubits is increased. This phenomenon becomes more pronounced once the number of qubits exceeds 6 after this number of qubits the probabilities are very close to zero. From our further calculations (which are not presented here), the probabilities of unmarked states vanish completely when the number of qubits is greater than 20 qubits.

In Fig.3, we display the behavior of the dynamical search of the probabilities of marked states ρ_{ege} and ρ_{geege} with the same dissipation rates. In the absence of dissipation, see Fig.2b and table (1), the probabilities of the current marked states or any other marked states at times $t_p = 0.04333\pi\hbar/\lambda\theta_4$ for 4 qubits and $t_p = 0.027065\pi\hbar/\lambda\theta_5$ for 5 qubits are 100% and the probabilities of un-marked states are zero. It is shown that when times are decreased from these values, the probabilities values of finding any marked states are less than 100% and decrease more and more according to the decreasing times. With these time decreases, the probabilities of finding any marked states are decreased and this decreasing is added to the un-marked states probabilities. This means that the revivals for the probabilities of un-marked states when the time is decreased more and more to become larger when the time is close to zero. However, when the time reaches zero, the probabilities of any marked or un-marked states are 6.25% and 3.125% for 4 and 5 qubits, respectively. This means that both marked and un-marked states have the same chance to contribute. In the presence of weak dissipation rate, one sees that the probabilities of current marked states in Fig.3a and Fig.3b or any other marked states at different values of the time are gradually decreased. The probabilities values of any desired state for any number of N at a weak values of similar dissipation are often close to each others. If the dissipation value is taken to be $\gamma_i = \lambda\theta_N$ ($i = 1, 2, \dots, N$), the probabilities values of any

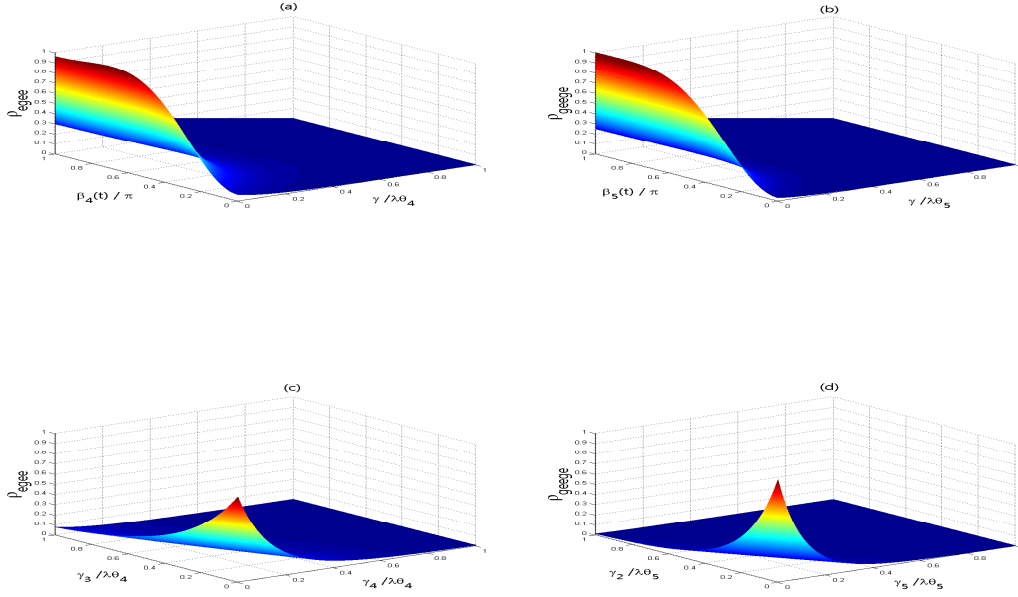


Figure 3: Dynamical quantum search algorithm for the probabilities of marked states ρ_{eeee} and ρ_{ggege} in the presence of dissipation, where $\gamma_i = \gamma$ ($i = 1, \dots, 4$) in (a); $\gamma_j = \gamma$ ($j = 1, \dots, 5$) in (b); $\gamma_1 = \gamma_2 = \gamma_4$ and $t_p = \frac{0.02813\pi\hbar}{\lambda\theta_4}$ in (c); $\gamma_1 = \gamma_3 = \gamma_5$, $\gamma_2 = \gamma_4$ and $t_p = \frac{0.027065\pi\hbar}{\lambda\theta_5}$ in (d).

desired state are sometimes increased or decreased to each other and one can not distinguish between the probability of any marked and un-marked states at any time. However, it is difficult to observe the probability of any marked state for any qubit at large dissipation rates, where small values of the probability of marked state is shown. Which means that both marked and un-marked states have the same chance to contribute.

Also, we display the behavior of the probabilities of current marked states in Fig.3c and Fig.3d for different values of qubits dissipation rates with time $t_p = 0.02813\pi\hbar/\lambda\theta_4$ for 4 qubits and $t_p = 0.027065\pi\hbar/\lambda\theta_5$ for 5 qubits. In the absence of dissipation the probabilities of any marked state for 4 qubits and 5 qubits at these values of times start from 0.8332 and from 1, respectively. When a weak value of qubits-dissipation is considered, one finds that the probabilities of the current states in Fig.3c and Fig.3d and any other marked states for 4 and 5 qubits are gradually decreased. The values of any desired states for 4 and 5 qubits in weak dissipation are often close to each other. It is shown that for strong dissipation, the probabilities of any marked states for 4 and 5 qubits are decreased further, while one can not distinguish between different probabilities of some un-marked states. It is interesting to mention here that the observation of any desired state will be more difficult when dissipation rate is equal to $\gamma_3 = \gamma_4 = \lambda\theta_4$ for 4 qubits and $\gamma_2 = \gamma_5 = \lambda\theta_5$ for 5 qubits or more than that, where there is some probabilities of un-marked states are larger than marked state. This means that both marked and un-marked states have the same chance to contribute.

However, the behavior of the probability of finding any remaining marked state for any different number of N in the dissipation presence, is similar to the previous behavior, see Fig.4. It is shown that, the time is a main factor in the appearance of different probabilities of marked states using different number of qubits. Therefore, the probabilities for the remaining marked states (3 states for 2 qubits, 7 states for 3 qubits, 14 states for 4 qubits, 29 states for 5 qubits and 63 states for 6 qubits) have the same behavior as in the figures displayed in the above.

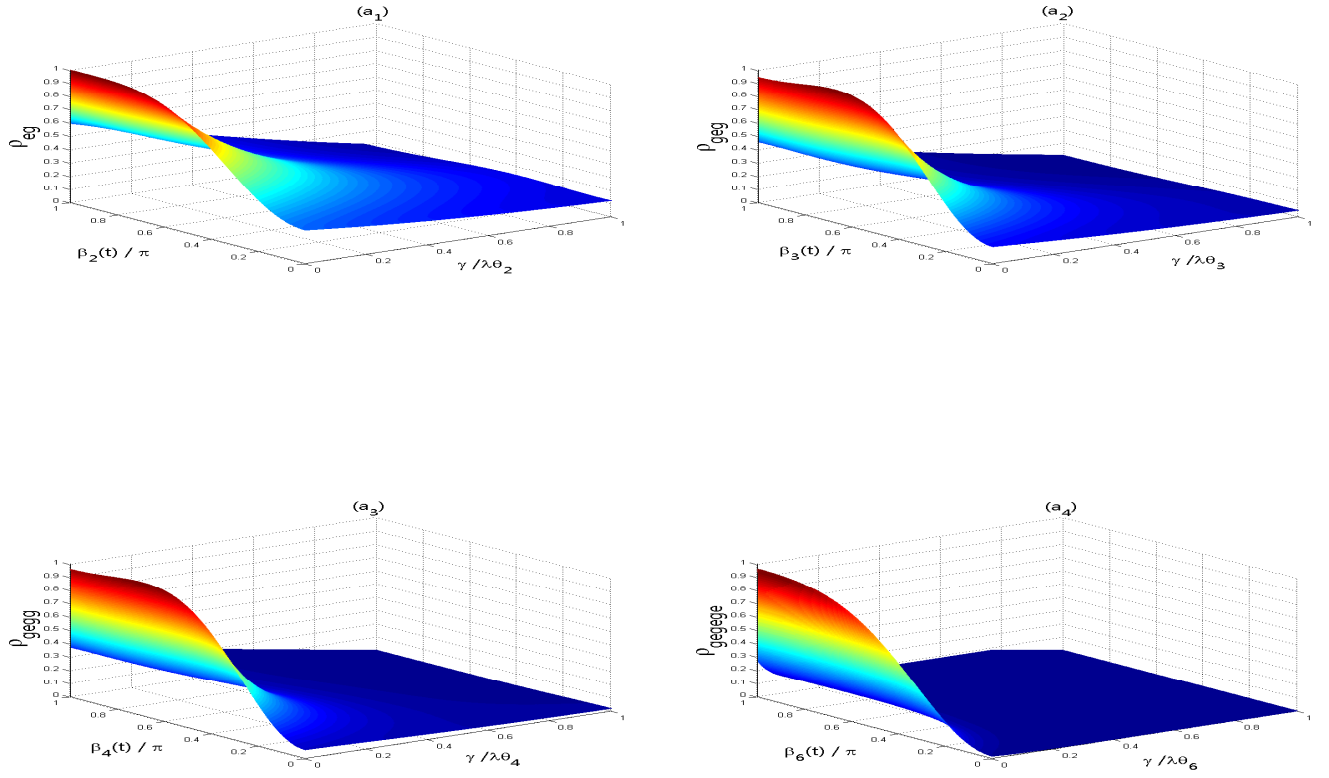


Figure 4: Dynamical quantum search algorithm for the probabilities of marked states ρ_{eg} , ρ_{geg} , ρ_{gegg} and ρ_{gegege} in the presence of similar dissipation rates.

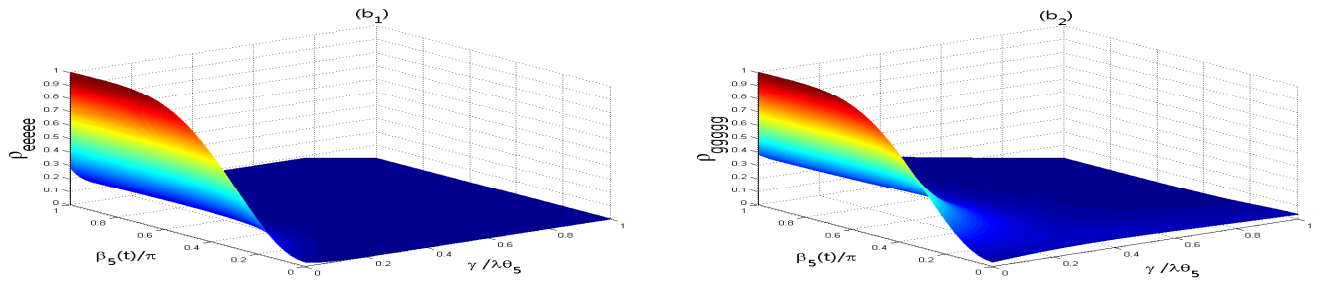


Figure 5: Dynamical quantum search algorithm with dissipation for 5 qubits to compare the values of ρ_{eeee} and ρ_{ggggg} .

In Fig.5, we plot DQSA for the probabilities ρ_{eeee} and ρ_{gggg} when the dissipation rates is considered. It is shown that the probabilities ρ_{gggg} and ρ_{eeee} are gradually decreased once dissipation rate takes small values, and the values of ρ_{eeee} are less than the values of ρ_{gggg} at any time. Also, one observes that the probability ρ_{gggg} is shown as larger values compared with the probability ρ_{eeee} which shows small values once dissipation rate $\gamma/\lambda\theta_5$ is increased. Therefore, we can distinguish the probability $\rho_{gg\dots g}$ for multi qubits at any time once dissipation rate is decreased or increased (or varied).

Now, we give a short discussion to observe un-marked states in the presence of dissipation rates either similar or different. The probabilities of un-desired states for weak dissipation are distinguished by a very small values and non-zero compared with the absence of dissipation. While for strong dissipation, the probability of the desired state is becoming less and is decreased due to the influence of strong dissipation and some of this decrease is added to the un-desired states. On the other hand, the results of finding any marked and un-marked states, in table (1) are completely in agreement with the results shown in Fig.3 and Fig.4, under the same conditions.

4 Conclusions

We have demonstrated on-demand generation of dynamic multi-qubit quantum search algorithm, which can be maintained for multi-qubit system. The algorithm we have demonstrated, gives favorable performance for multi-qubit (up to 9 qubits) and would survive even in the presence of the qubit dissipation. We have focused our attention on the probabilities of the first 9 qubits and have obtained that their optimal values come either to diagonalizing or to symmetrizing probabilities, that implies analytical formula for its calculation. Comparing these results with Grover algorithm analysis allows to give a similar result when the number of involved qubits get much larger, and is an example of a perfect observation which is suitable for a particular purpose, e.g., for the time dependent interaction and dissipation processes. The long life time of this multi-qubit algorithm is due to a high symmetry of the generated forms. We have used different values of the controlled phase to improve the suggested algorithm performance. A new technique is used to generate the dynamical quantum gates that helps in implementing the current algorithm. The multi-qubit character of the interaction used for the creation of dynamical algorithm allows for the potential applications and extension of the present method to other models, possibly including, superconducting materials or solid state models with long lived spin states.

Appendix

In this appendix, we took four optional values of times (say, $\frac{0.331\pi\hbar}{2^N\lambda\theta_N}$, $\frac{0.566\pi\hbar}{2^N\lambda\theta_N}$, t_{Np} and $\frac{\pi\hbar}{2^N\lambda\theta_N}$) to calculate the probabilities of some marked and unmarked states for different number of N . The time t_{Np} gives the highest probabilities for marked states with different values of N .

First, it is easy to see that the sum of all probabilities for all marked and unmarked states at any time in the absence of dissipation rates is equal to one, see Fig.2. Also, from Figs.3, Fig.4, Fig.5 and the above tables, one can note that the sum of all probabilities in the presence of dissipation at different times are gradually decreased than one, and reaches almost zero at high values of dissipation rates.

Second, from Tables (2-11), one observes and distinguishes between different values of times for the probabilities of each marked state at weak values of the dissipation rates. Moreover, we observe for times t_{Np} , and a weak dissipation, that the probabilities of each marked states have

Times	$t = \frac{0.331\pi\hbar}{4\lambda\theta_2}$	$t = \frac{0.566\pi\hbar}{4\lambda\theta_2}$	$t_{2p} = \frac{0.9425\pi\hbar}{4\lambda\theta_2}$	$t = \frac{\pi\hbar}{4\lambda\theta_2}$
ρ_{ee}	0.5583	0.8537	0.9625	0.9618
Pr. r. s.	0.1417, 0.1411, 0.1427	0.0407, 0.0405, 0.0397	1.5605e, 1.5524e, 1.7800d	7.7440d, 7.5690d, 0
ρ_{ge}	0.5634	0.8595	0.9668	0.9659
Pr. r. s.	0.1389, 0.1405, 0.1428	0.0399, 0.0390, 0.0399	1.5556e, 1.6690d, 2.5570d	7.5690d, 0, 1.0000c
ρ_{gg}	0.5697	0.8667	0.9722	0.9712
Pr. r. s.	0.1378, 0.1404, 0.1401	0.0382, 0.0388, 0.0390	1.6490d, 9.6400c, 2.5700d	0, 1.0000c, 1.0000c

Table 2: Outputs of dynamical quantum search algorithm for some probabilities of marked states $\rho_{r_1 r_2}$ ($r_1, r_2 = e, g$) and unmarked states or remaining states (Pr. r. s.) of 2-qubit for different values of time, where $\frac{\gamma_1}{\lambda} = \frac{\theta_2}{113}$ and $\frac{\gamma_2}{\lambda} = \frac{\theta_2}{90}$; $c = \times 10^{-6}$, $d = \times 10^{-5}$ and $e = \times 10^{-4}$.

Times	$t = \frac{0.331\pi\hbar}{4\lambda\theta_2}$	$t = \frac{0.566\pi\hbar}{4\lambda\theta_2}$	$t_{2p} = \frac{0.9425\pi\hbar}{4\lambda\theta_2}$	$t = \frac{\pi\hbar}{4\lambda\theta_2}$
ρ_{ee}	0.0961	0.1224	0.1142	0.1108
Pr. r. s.	0.0921, 0.0933, 0.1792	0.0625, 0.0632, 0.0680	0.0428, 0.0434, 0.0049	0.0426, 0.0432, 0.0043
ρ_{ge}	0.1683	0.1700	0.1148	0.1089
Pr. r. s.	0.0528, 0.0699, 0.1660	0.0491, 0.0248, 0.0486	0.0333, 0.0041, 5.7600e	0.0329, 0.0040, 3.1329e
ρ_{gg}	0.3244	0.2640	0.1098	0.0997
Pr. r. s.	0.0308, 0.0713, 0.0712	0.0127, 0.0251, 0.0239	0.0021, 3.2962e, 3.4306e	0.0021, 1.7640d, 9.2160d

Table 3: The same as Table (2) but $\frac{\gamma_1}{\lambda} = \frac{4\theta_2}{5}$ and $\frac{\gamma_2}{\lambda} = \frac{7\theta_2}{9}$.

Times	$t = \frac{0.331\pi\hbar}{8\lambda\theta_3}$	$t = \frac{0.566\pi\hbar}{8\lambda\theta_3}$	$t_{3p} = \frac{0.6723\pi\hbar}{8\lambda\theta_3}$	$t = \frac{\pi\hbar}{8\lambda\theta_3}$
ρ_{eee}	0.5989	0.9085	0.9348	0.8776
Pr. r. s.	0.0520, 0.0524, 0.0516, 0.0522, 0.0516, 0.0517, 0.0518	0.0052, 0.0053, 0.0046, 0.0052, 0.0047, 0.0046, 0.0044	1.0345e, 1.1197e, 4.1220d, 1.0625e, 4.5460d, 3.7480d, 2.5210d	0.0064, 0.0063, 0.0064, 0.0064, 0.0065, 0.0064, 0.0063
ρ_{eeg}	0.6051	0.9170	0.9435	0.8855
Pr. r. s.	0.0515, 0.0512, 0.0522, 0.0511, 0.0520, 0.0513, 0.0515	0.0052, 0.0046, 0.0049, 0.0047, 0.0048, 0.0044, 0.0042	9.5290d, 3.6000d, 5.9300d, 4.1780d, 5.6250d, 2.1130d, 1.3220d	0.0068, 0.0068, 0.0065, 0.0069, 0.0066, 0.0067, 0.0065
ρ_{ege}	0.6085	0.9218	0.9483	0.8898
Pr. r. s.	0.0517, 0.0509, 0.0517, 0.0509, 0.0511, 0.0519, 0.0513	0.0053, 0.0046, 0.0046, 0.0046, 0.0044, 0.0046, 0.0041	9.8960d, 3.4340d, 3.4490d, 3.0920d, 1.9240d, 3.6170d, 8.8400c	0.0069, 0.0070, 0.0067, 0.0070, 0.0069, 0.0067, 0.0067
ρ_{gee}	0.6065	0.9191	0.9454	0.8874
Pr. r. s.	0.0516, 0.0510, 0.0511, 0.0512, 0.0518, 0.0522, 0.0514	0.0052, 0.0047, 0.0046, 0.0044, 0.0047, 0.0048, 0.0041	9.6260d, 4.0000d, 3.2500d, 2.0500d, 4.4680d, 5.0500d, 1.1250d	0.0069, 0.0069, 0.0069, 0.0068, 0.0067, 0.0065, 0.0066
ρ_{gge}	0.6162	0.9325	0.9590	0.8998
Pr. r. s.	0.0504, 0.0505, 0.0513, 0.0507, 0.0515, 0.0507, 0.0515	0.0046, 0.0044, 0.0046, 0.0041, 0.0048, 0.0041, 0.0041	2.4820d, 1.5170d, 3.0440d, 6.6100c, 4.1810d, 7.7600c, 9.9700c	0.0075, 0.0074, 0.0071, 0.0072, 0.0071, 0.0072, 0.0069

Table 4: Outputs of dynamical quantum search algorithm for some probabilities of marked states $\rho_{r_1 r_2 r_3}$ ($r_1, r_2, r_3 = e, g$) and unmarked states of 3-qubit for different values of time, where $\frac{\gamma_1}{\lambda} = \frac{\theta_3}{113}$, $\frac{\gamma_2}{\lambda} = \frac{\theta_3}{90}$ and $\frac{\gamma_3}{\lambda} = \frac{\theta_3}{140}$.

Times	$t = \frac{0.331\pi\hbar}{8\lambda\theta_3}$	$t = \frac{0.566\pi\hbar}{8\lambda\theta_3}$	$t_{3p} = \frac{0.6723\pi\hbar}{8\lambda\theta_3}$	$t = \frac{\pi\hbar}{8\lambda\theta_3}$
ρ_{eee}	0.0217	0.0234	0.0201	0.0113
Pr. r. s.	0.0183, 0.0201, 0.0257, 0.0204, 0.0261, 0.0289, 0.0596	0.0129, 0.0140, 0.0088, 0.0142, 0.0089, 0.0094, 0.0044	0.0093, 0.0100, 0.0054, 0.0101, 0.0054, 0.0055, 4.8420e	0.0033, 0.0034, 0.0026, 0.0034, 0.0026, 0.0023, 0.0051
ρ_{eeg}	0.0317	0.0297	0.0247	0.0135
Pr. r. s.	0.0145, 0.0160, 0.0256, 0.0162, 0.0261, 0.0238, 0.0539	0.0109, 0.0085, 0.0085, 0.0086, 0.0087, 0.0050, 0.0027	0.0072, 0.0051, 0.0051, 0.0051, 0.0052, 0.0024, 2.6240d	0.0018, 7.9524e, 0.0023, 7.7284e, 0.0023, 9.2416e, 0.0030
ρ_{ege}	0.0356	0.0327	0.0268	0.0140
Pr. r. s.	0.0152, 0.0146, 0.0241, 0.0161, 0.0207, 0.0282, 0.0520	0.0111, 0.0075, 0.0071, 0.0081, 0.0042, 0.0084, 0.0022	0.0072, 0.0043, 0.0040, 0.0045, 0.0019, 0.0047, 2.3050d	0.0017, 5.8564e, 0.0016, 4.7089e, 7.2900e, 0.0016, 0.0026
ρ_{gee}	0.0362	0.0332	0.0271	0.0141
Pr. r. s.	0.0153, 0.0145, 0.0159, 0.0203, 0.0243, 0.0279, 0.0518	0.0112, 0.0074, 0.0079, 0.0040, 0.0070, 0.0082, 0.0022	0.0073, 0.0042, 0.0044, 0.0018, 0.0039, 0.0045, 3.1760d	0.0016, 5.4289e, 4.4521e, 7.0225e, 0.0015, 0.0015, 0.0025
ρ_{gge}	0.0737	0.0571	0.0448	0.0213
Pr. r. s.	0.0105, 0.0097, 0.0193, 0.0152, 0.0192, 0.0153, 0.0420	0.0045, 0.0026, 0.0087, 0.0010, 0.0085, 9.8881e, 1.7730e	0.0017, 7.9322e, 0.0041, 2.4912e, 0.0039, 2.3850e, 9.4625e	2.7040d, 5.1840d, 1.4161e, 4.8400c, 1.2100e, 5.7600c, 0.0014

Table 5: The same as Table (4) but $\frac{\gamma_1}{\lambda} = \frac{4\theta_3}{5}$, $\frac{\gamma_2}{\lambda} = \frac{7\theta_3}{9}$ and $\frac{\gamma_3}{\lambda} = \frac{5\theta_3}{8}$.

Times	$t = \frac{0.331\pi\hbar}{16\lambda\theta_4}$	$t = \frac{0.566\pi\hbar}{16\lambda\theta_4}$	$t_{4p} = \frac{0.6933\pi\hbar}{16\lambda\theta_4}$	$t = \frac{\pi\hbar}{16\lambda\theta_4}$
ρ_{eeee}	0.5433	0.8570	0.8900	0.8499
Pr. r. s.	0.0269, 0.0267, 0.0259, 0.0269, 0.0258, 0.0259, 0.0256, 0.0268, 0.0259, 0.0259, 0.0256, 0.0258, 0.0255, 0.0256, 0.0253	0.0032, 0.0032, 0.0030, 0.0033, 0.0030, 0.0030, 0.0030, 0.0032, 0.0030, 0.0030, 0.0030, 0.0030, 0.0030, 0.0030, 0.0029	6.5530d, 5.7800d, 5.3210d, 6.9200d, 5.7250d, 5.4500d, 6.3610d, 6.3370d, 5.5210d, 5.2520d, 6.1450d, 5.5210d, 6.5810d, 6.2820d, 7.2650d	0.0016, 0.0016, 0.0018, 0.0016, 0.0018, 0.0018, 0.0019, 0.0016, 0.0018, 0.0018, 0.0019, 0.0018, 0.0019, 0.0019, 0.0020
ρ_{eegg}	0.5611	0.8840	0.9178	0.8767
Pr. r. s.	0.0260, 0.0262, 0.0265, 0.0257, 0.0254, 0.0255, 0.0260, 0.0257, 0.0254, 0.0255, 0.0259, 0.0254, 0.0251, 0.0252, 0.0248	0.0028, 0.0029, 0.0030, 0.0028, 0.0027, 0.0028, 0.0029, 0.0028, 0.0027, 0.0028, 0.0029, 0.0027, 0.0027, 0.0027, 0.0027	1.3220d, 2.5780d, 2.8090d, 1.8010d, 2.3840d, 2.1730d, 4.4690d, 1.6850d, 2.3050d, 2.0450d, 3.9290d, 2.3050d, 3.0250d, 2.7250d, 3.5050d	0.0020, 0.0019, 0.0018, 0.0020, 0.0021, 0.0021, 0.0020, 0.0020, 0.0021, 0.0021, 0.0020, 0.0021, 0.0022, 0.0022, 0.0023
ρ_{eggg}	0.5729	0.9019	0.9364	0.8947
Pr. r. s.	0.0257, 0.0254, 0.0255, 0.0260, 0.0254, 0.0256, 0.0259, 0.0254, 0.0251, 0.0252, 0.0249, 0.0251, 0.0248, 0.0249, 0.0253	0.0027, 0.0026, 0.0026, 0.0028, 0.0026, 0.0027, 0.0028, 0.0026, 0.0026, 0.0026, 0.0026, 0.0026, 0.0026, 0.0026, 0.0027	3.9200c, 6.4800c, 5.4500c, 1.8180d, 6.8500c, 1.6290d, 1.8180d, 6.1300c, 9.2500c, 8.4100c, 1.2010d, 1.0130d, 1.4050d, 1.3010d, 2.8250d	0.0022, 0.0022, 0.0022, 0.0021, 0.0023, 0.0022, 0.0021, 0.0022, 0.0023, 0.0023, 0.0024, 0.0023, 0.0024, 0.0024, 0.0023
ρ_{geeg}	0.5629	0.8867	0.9206	0.8795
Pr. r. s.	0.0259, 0.0263, 0.0257, 0.0254, 0.0045, 0.0042, 0.0055, 0.0038, 0.0046, 0.0042, 0.0056, 0.0047, 0.0064, 0.0057, 0.0153	0.0028, 0.0029, 0.0028, 0.0027, 0.0028, 0.0015, 0.0011, 0.0018, 0.0016, 0.0015, 0.0011, 0.0016, 0.0010, 0.0011, 4.9361e	1.1450d, 2.5480d, 1.4450d, 1.9010d, 1.6180d, 2.1530d, 1.9720d, 2.5610d, 2.6330d, 1.8500d, 3.3650d, 2.0250d, 4.2530d, 2.5000d, 3.1610d	0.0020, 0.0019, 0.0020, 0.0021, 0.0021, 0.0021, 0.0021, 0.0021, 0.0019, 0.0021, 0.0021, 0.0022, 0.0021, 0.0022, 0.0023

Table 6: Outputs of dynamical quantum search algorithm for some probabilities of marked states $\rho_{r_1 r_2 r_3 r_4}$ ($r_1, r_2, r_3, r_4 = e, g$) and unmarked states of 4-qubit for different values of time, where $\frac{\gamma_1}{\lambda} = \frac{\theta_4}{113}$, $\frac{\gamma_2}{\lambda} = \frac{\theta_4}{90}$, $\frac{\gamma_3}{\lambda} = \frac{\theta_4}{140}$ and $\frac{\gamma_4}{\lambda} = \frac{\theta_4}{100}$.

Times	$t = \frac{0.331\pi\hbar}{16\lambda\theta_4}$	$t = \frac{0.566\pi\hbar}{16\lambda\theta_4}$	$t_{4p} = \frac{0.6933\pi\hbar}{16\lambda\theta_4}$	$t = \frac{\pi\hbar}{16\lambda\theta_4}$
ρ_{eeee}	0.0034	0.0025	0.0018	0.0017
Pr. r. s.	0.0038, 0.0035, 0.0041, 0.0038, 0.0045, 0.0042, 0.0055, 0.0038, 0.0046, 0.0042, 0.0056, 0.0047, 0.0064, 0.0057, 0.0153	0.0017, 0.0016, 0.0015, 0.0017, 0.0016, 0.0015, 0.0011, 0.0018, 0.0016, 0.0015, 0.0011, 0.0016, 0.0010, 0.0011, 4.9361e	9.1801e, 8.9317e, 8.3357e, 9.2909e, 8.0002e, 8.2450e, 0.0011, 9.3466e, 7.9141e, 8.2273e, 0.0011, 7.8829e, 9.7501e, 0.0010, 0.0025	0.0010, 9.6100e, 7.7284e, 0.0010, 8.0089e, 7.7841e, 4.2025e, 0.0010, 8.0089e, 7.7841e, 4.2436e, 8.0656e, 4.4944e, 4.3264e, 1.0000 $\times 10^{-8}$
ρ_{eegg}	0.0071	0.0048	0.0037	0.0026
Pr. r. s.	0.0024, 0.0035, 0.0035, 0.0029, 0.0037, 0.0035, 0.0049, 0.0030, 0.0037, 0.0035, 0.0050, 0.0034, 0.0047, 0.0043, 0.0127	7.7860e, 0.0012, 0.0012, 8.0725e, 8.3394e, 8.4361e, 0.0010, 8.0770e, 8.3449e, 8.4817e, 0.0010, 7.5393e, 4.4753e, 4.8322e, 6.1274e	3.1058e, 4.9130e, 5.4666e, 2.7961e, 3.2020e, 3.4613e, 9.2273e, 2.7505e, 3.1720e, 3.4289e, 9.1705e, 3.0266e, 4.9689e, 5.3170e, 0.0018	4.0000e, 5.6169e, 5.8081e, 4.0000e, 3.4225e, 3.3489e, 2.5281e, 4.0000e, 3.4596e, 3.3856e, 2.6244e, 3.2761e, 1.1881e, 1.1449e, 8.4640d
ρ_{eggg}	0.0148	0.0100	0.0079	0.0044
Pr. r. s.	0.0019, 0.0026, 0.0025, 0.0045, 0.0026, 0.0043, 0.0044, 0.0023, 0.0025, 0.0024, 0.0033, 0.0025, 0.0036, 0.0034, 0.0095	4.1785e, 4.9360e, 5.0265e, 0.0011, 4.9034e, 9.2489e, 0.0010, 4.3810e, 3.8849e, 3.9641e, 3.4597e, 3.8628e, 3.0980e, 3.3857e, 0.0012	1.3136e, 1.2770e, 1.3549e, 4.2365e, 1.2456e, 3.3808e, 4.0637e, 1.3130e, 1.4257e, 1.4788e, 3.0025e, 1.3925e, 2.9314e, 2.9786e, 0.0019	1.2100e, 1.2996e, 1.2996e, 2.9584e, 1.2996e, 2.4649e, 2.8900e, 1.0816e, 6.5610d, 6.5610d, 4.0000c, 6.5610d, 2.8900c, 4.0000c, 4.9000d
ρ_{geeg}	0.0084	0.0054	0.0041	0.0029
Pr. r. s.	0.0024, 0.0037, 0.0026, 0.0032, 0.0029, 0.0037, 0.0029, 0.0038, 0.0038, 0.0033, 0.0046, 0.0038, 0.0056, 0.0040, 0.0122	7.0922e, 0.0012, 6.8965e, 7.2320e, 7.0381e, 7.4378e, 6.4129e, 4.2530e, 0.0012, 7.2041e, 8.5426e, 7.4321e, 9.0625e, 4.1474e, 7.2585e	2.6185e, 4.9985e, 2.3620e, 2.8793e, 2.1853e, 2.5348e, 2.7625e, 4.9369e, 4.7890e, 2.7716e, 7.7681e, 2.4500e, 7.5024e, 4.7545e, 0.0018	3.4596e, 5.5696e, 3.2761e, 2.7225e, 3.4225e, 2.9584e, 2.5921e, 7.5690d, 5.4756e, 2.7556e, 1.8496e, 2.9929e, 2.4025e, 7.9210d, 1.2769e
ρ_{ggeg}	0.0195	0.0125	0.0095	0.0054
Pr. r. s.	0.0018, 0.0026, 0.0019, 0.0020, 0.0027, 0.0051, 0.0021, 0.0027, 0.0027, 0.0051, 0.0021, 0.0027, 0.0050, 0.0028, 0.0083	3.2786e, 3.9785e, 3.4632e, 3.2057e, 3.9469e, 0.0010, 3.2050e, 3.3730e, 3.9469e, 0.0010, 3.1688e, 3.3377e, 9.7604e, 3.2677e, 0.0014	9.8410d, 8.8650d, 1.1365e, 1.2874e, 8.6210d, 3.5257e, 1.2789e, 2.8346e, 8.5520d, 3.3962e, 1.2580e, 2.8157e, 3.2185e, 2.7693e, 0.0019	7.9210d, 9.0250d, 6.2410d, 2.9160d, 9.0250d, 2.7556e, 2.9160d, 1.4400c, 9.0250d, 2.6569e, 2.9160d, 1.4400c, 2.5921e, 1.4400c, 1.5625e

Table 7: The same as Table (6) but $\frac{\gamma_1}{\lambda} = \frac{4\theta_4}{5}$, $\frac{\gamma_2}{\lambda} = \frac{7\theta_4}{9}$, $\frac{\gamma_3}{\lambda} = \frac{5\theta_4}{8}$ and $\frac{\gamma_4}{\lambda} = \frac{3\theta_4}{4}$.

Times	$t = \frac{0.331\pi\hbar}{32\lambda\theta_5}$	$t = \frac{0.566\pi\hbar}{32\lambda\theta_5}$	$t_{5p} = \frac{0.8661\pi\hbar}{32\lambda\theta_5}$	$t = \frac{\pi\hbar}{32\lambda\theta_5}$
ρ_{eeeeeg}	0.4478	0.7707	0.8562	0.8536
Pr. r. s.	0.0159, 0.0153, 0.0156, 0.0153, 0.0155, 0.0151, 0.0149, 0.0152, 0.0156, 0.0150, 0.0148, 0.0151, 0.0149, 0.0148, 0.0146, 0.0153, 0.0156, 0.0150, 0.0149, 0.0151, 0.0149, 0.0149, 0.0147, 0.0150, 0.0148, 0.0148, 0.0146, 0.0149, 0.0146, 0.0146, 0.0144	0.0035, 0.0035, 0.0037, 0.0035, 0.0036, 0.0035, 0.0035, 0.0035, 0.0037, 0.0035, 0.0036, 0.0035, 0.0036, 0.0036, 0.0036, 0.0035, 0.0036, 0.0035, 0.0036, 0.0035, 0.0035, 0.0036, 0.0036, 0.0035, 0.0036, 0.0036, 0.0036, 0.0036, 0.0036, 0.0036, 0.0037	{ 5.9130, 3.9610, 5.5840, 4.1210, 5.1610, 3.7060, 3.4850, 3.9240, 5.8760, 3.6500, 3.4640, 3.7060, 3.4850, 3.4640, 3.2850, 3.9610, 5.4410, 3.7060, 3.4850, 3.7370, 3.5080, 3.4850, 3.2980, 3.6770, 3.4640, 3.4450, 3.2740, 3.4640, 3.2850, 3.2740, 3.1370}d	1.0000a, 1.6000b, 8.1000b, 2.5000b, 2.5000b, 4.0000a, 1.0000a, 1.6000b, 1.2100c, 0, 9.0000a, 1.0000a, 4.0000a, 9.0000a, 3.6000b, 2.5000b, 6.4000b, 1.0000a, 4.0000a, 4.0000a, 1.0000a, 4.0000a, 2.5000b, 1.0000a, 4.0000a, 9.0000a, 4.9000b, 4.0000a, 2.5000b, 3.6000b, 1.0000c
ρ_{eeeg}	0.4553	0.7835	0.8707	0.8683
Pr. r. s.	0.0154, 0.0156, 0.0152, 0.0150, 0.0157, 0.0150, 0.0153, 0.0152, 0.0150, 0.0149, 0.0147, 0.0150, 0.0154, 0.0147, 0.0145, 0.0152, 0.0150, 0.0150, 0.0148, 0.0150, 0.0153, 0.0148, 0.0146, 0.0149, 0.0147, 0.0147, 0.0145, 0.0148, 0.0146, 0.0145, 0.0143	0.0033, 0.0035, 0.0034, 0.0034, 0.0035, 0.0034, 0.0036, 0.0034, 0.0034, 0.0035, 0.0035, 0.0034, 0.0036, 0.0035, 0.0035, 0.0034, 0.0034, 0.0034, 0.0035, 0.0034, 0.0036, 0.0035, 0.0035, 0.0034, 0.0035, 0.0035, 0.0035, 0.0035, 0.0035, 0.0035, 0.0036	{ 3.1040, 4.1210, 2.857, 2.6440, 4.2850, 2.6690, 4.0400, 2.8260, 4.6450, 2.5220, 2.3530, 2.6440, 4.1650, 2.3530, 2.2180, 2.8570, 2.6690, 2.6440, 2.4650, 2.6690, 3.9170, 2.4650, 2.3200, 2.6210, 2.4500, 2.3400, 2.2130, 2.4650, 2.3200, 2.2130, 2.1200}d	3.2400c, 4.9000b, 1.9600c, 1.4400c, 4.9000b, 1.4400c, 4.0000a, 1.9600c, 9.0000a, 3.6000b, 1.0000a, 4.0000a, 1.6000b, 4.9000b, 1.6000b, 2.2500c, 1.4400c, 1.2100c, 6.4000b, 1.4400c, 0, 6.4000b, 2.5000b, 1.2100c, 6.4000b, 4.9000b, 9.0000a, 6.4000b, 2.5000b, 1.6000b, 0
ρ_{egeee}	0.4510	0.7761	0.8623	0.8597
Pr. r. s.	0.0161, 0.0153, 0.0152, 0.0150, 0.0153, 0.0151, 0.0150, 0.0149, 0.0154, 0.0155, 0.0148, 0.0154, 0.0148, 0.0148, 0.0146, 0.0153, 0.0151, 0.0150, 0.0148, 0.0151, 0.0149, 0.0148, 0.0146, 0.0155, 0.0148, 0.0147, 0.0145, 0.0148, 0.0146, 0.0145, 0.0143	0.0036, 0.0034, 0.0034, 0.0035, 0.0034, 0.0035, 0.0035, 0.0035, 0.0036, 0.0036, 0.0035, 0.0036, 0.0035, 0.0035, 0.0036, 0.0034, 0.0035, 0.0035, 0.0035, 0.0035, 0.0035, 0.0035, 0.0036, 0.0036, 0.0035, 0.0035, 0.0036, 0.0035, 0.0036, 0.0036, 0.0036	{ 5.9680, 3.5730, 3.4600, 3.2210, 3.6100, 3.3610, 3.2210, 3.0160, 4.6450, 4.9130, 2.9800, 4.5140, 3.0160, 2.9970, 2.8340, 3.4600, 3.2210, 3.1940, 2.9970, 3.3610, 3.0370, 3.0160, 2.8450, 4.7780, 2.9970, 2.9800, 2.8250, 2.9970, 2.8340, 2.8250, 2.7040}d	0, 8.1000b, 8.1000b, 3.6000b, 1.0000c, 4.9000b, 3.6000b, 9.0000a, 9.0000a, 3.6000b, 1.0000a, 4.0000a, 4.0000a, 4.0000a, 4.0000a, 8.1000b, 3.6000b, 2.5000b, 4.0000a, 3.6000b, 9.0000a, 9.0000a, 1.0000a, 2.5000b, 4.0000a, 1.0000a, 4.0000a, 4.0000a, 1.0000a, 4.0000a, 3.6000b
ρ_{egegg}	0.4704	0.8088	0.8987	0.8962
Pr. r. s.	0.0152, 0.0151, 0.0150, 0.0154, 0.0151, 0.0149, 0.0148, 0.0146, 0.0150, 0.0153, 0.0152, 0.0148, 0.0146, 0.0145, 0.0147, 0.0150, 0.0148, 0.0148, 0.0146, 0.0149, 0.0147, 0.0146, 0.0144, 0.0148, 0.0146, 0.0145, 0.0148, 0.0146, 0.0144, 0.0143, 0.0141	0.0032, 0.0032, 0.0032, 0.0034, 0.0032, 0.0033, 0.0033, 0.0033, 0.0032, 0.0034, 0.0034, 0.0033, 0.0033, 0.0033, 0.0035, 0.0032, 0.0033, 0.0033, 0.0033, 0.0033, 0.0033, 0.0033, 0.0034, 0.0033, 0.0033, 0.0033, 0.0035, 0.0033, 0.0034, 0.0034, 0.0034	1.3810d, 1.2100d, 1.2100d, 2.3780d, 1.3000d, 1.1530d, 1.0730d, 9.7000c, 1.1890d, 2.1460d, 1.8450d, 1.0730d, 9.7000c, 9.6500c, 1.5220d, 1.2100d, 1.0730d, 1.0600d, 9.6500c, 1.0880d, 9.7700c, 9.7000c, 9.0100c, 1.0600d, 9.6500c, 9.6200c, 1.6820d, 9.6500c, 9.0400c, 9.0900c, 8.3300c	1.3690d, 1.1560d, 1.0890d, 3.2400c, 1.1560d, 9.6100c, 9.6100c, 7.8400c, 1.0890d, 3.6100c, 4.0000c, 9.0000c, 7.2900c, 6.7600c, 2.2500c, 1.1560d, 9.6100c, 9.0000c, 7.2900c, 9.6100c, 7.8400c, 7.2900c, 5.7600c, 9.0000c, 6.7600c, 6.7600c, 1.6900c, 7.2900c, 5.7600c, 5.2900c, 3.6100c
ρ_{geeee}	0.4486	0.7721	0.8578	0.8553
Pr. r. s.	0.0160, 0.0153, 0.0153, 0.0151, 0.0153, 0.0151, 0.0151, 0.0149, 0.0152, 0.0150, 0.0150, 0.0148, 0.0151, 0.0149, 0.0148, 0.0146, 0.0155, 0.0156, 0.0149, 0.0155, 0.0149, 0.0149, 0.0147, 0.0156, 0.0148, 0.0148, 0.0146, 0.0148, 0.0146, 0.0146, 0.0144	0.0035, 0.0034, 0.0035, 0.0035, 0.0034, 0.0035, 0.0035, 0.0035, 0.0035, 0.0035, 0.0035, 0.0036, 0.0035, 0.0035, 0.0036, 0.0036, 0.0036, 0.0037, 0.0035, 0.0036, 0.0035, 0.0035, 0.0036, 0.0037, 0.0036, 0.0036, 0.0036, 0.0035, 0.0036, 0.0036, 0.0037	{ 5.9130, 3.8420, 3.8050, 3.5890, 3.8810, 3.6200, 3.5890, 3.3700, 3.8050, 3.5600, 3.5330, 3.3300, 3.5600, 3.3700, 3.3490, 3.1610, 5.1220, 5.4020, 3.3490, 4.9850, 3.3930, 3.3700, 3.1850, 5.5450, 3.3490, 3.3300, 3.0500, 3.3490, 3.1720, 3.1610, 3.0260 }d	1.0000a, 3.6000b, 3.6000b, 9.0000a, 4.9000b, 1.6000b, 9.0000a, 0, 2.5000b, 4.0000a, 1.0000a, 4.0000a, 4.0000a, 1.0000a, 1.0000a, 2.5000b, 3.6000b, 8.1000b, 1.0000a, 1.6000b, 0, 0, 1.6000b, 1.0000c, 1.0000a, 4.0000a, 2.5000b, 1.0000a, 1.6000b, 2.5000b, 8.1000b
ρ_{gegeg}	0.4647	0.7993	0.8881	0.8857
Pr. r. s.	0.0153, 0.0151, 0.0151, 0.0149, 0.0151, 0.0154, 0.0149, 0.0147, 0.0150, 0.0148, 0.0148, 0.0146, 0.0149, 0.0147, 0.0146, 0.0144, 0.0151, 0.0153, 0.0149, 0.0147, 0.0154, 0.0147, 0.0150, 0.0148, 0.0146, 0.0146, 0.0144, 0.0146, 0.0150, 0.0144, 0.0142	0.0033, 0.0033, 0.0033, 0.0033, 0.0033, 0.0035, 0.0033, 0.0034, 0.0033, 0.0034, 0.0033, 0.0034, 0.0033, 0.0034, 0.0034, 0.0034, 0.0033, 0.0034, 0.0033, 0.0034, 0.0034, 0.0034, 0.0036, 0.0034, 0.0034, 0.0034, 0.0035, 0.0034, 0.0036, 0.0035, 0.0035	{ 1.9700, 1.7690, 1.7440, 1.6020, 1.7960, 2.8260, 1.6020, 1.4690, 1.7440, 1.5850, 1.4930, 1.3780, 1.6020, 1.4690, 1.3850, 1.2970, 1.7690, 2.4730, 1.5850, 1.4600, 2.6960, 1.4690, 2.5360, 1.5080, 1.3850, 1.3780, 1.2970, 1.4600, 2.6370, 1.2970, 1.2500}d	9.0000c, 7.2900c, 6.7600c, 5.2900c, 7.2900c, 1.9600c, 5.7600c, 4.4100c, 6.7600c, 5.2900c, 4.8400c, 3.6100c, 5.2900c, 4.0000c, 3.6100c, 2.5600c, 7.2900c, 2.5600c, 5.2900c, 4.0000c, 2.2500c, 4.0000c, 3.6000b, 5.2900c, 3.6100c, 3.6100c, 2.2500c, 4.0000c, 1.6000b, 2.5600c, 1.4400c
ρ_{ggegg}	0.4712	0.8104	0.9004	0.8979
Pr. r. s.	0.0152, 0.0150, 0.0150, 0.0148, 0.0151, 0.0149, 0.0148, 0.0146, 0.0150, 0.0148, 0.0152, 0.0145, 0.0148, 0.0146, 0.0145, 0.0143, 0.0150, 0.0148, 0.0154, 0.0146, 0.0149, 0.0147, 0.0146, 0.0144, 0.0153, 0.0145, 0.0147, 0.0146, 0.0144, 0.0147, 0.0141	0.0032, 0.0032, 0.0032, 0.0033, 0.0032, 0.0033, 0.0033, 0.0033, 0.0032, 0.0033, 0.0034, 0.0033, 0.0033, 0.0033, 0.0033, 0.0034, 0.0032, 0.0033, 0.0034, 0.0033, 0.0033, 0.0033, 0.0033, 0.0034, 0.0034, 0.0033, 0.0035, 0.0033, 0.0034, 0.0033, 0.0035, 0.0033, 0.0034, 0.0035, 0.0034	1.3140d, 1.1450d, 1.1240d, 9.9700c, 1.1450d, 1.0250d, 1.0100d, 9.0900c, 1.1240d, 9.9700c, 1.9490d, 9.0100c, 9.9700c, 9.0400c, 9.0100c, 8.5000c, 1.1450d, 1.0100d, 2.2600d, 9.0400c, 1.0100d, 9.0900c, 9.0400c, 8.4500c, 2.0570d, 9.0100c, 1.5220d, 9.0400c, 8.4500c, 1.4450d, 7.9300c	1.4440d, 1.2250d, 1.2250d, 1.0240d, 1.2250d, 1.0890d, 1.0240d, 8.4100c, 1.1560d, 9.6100c, 4.4100c, 7.2900c, 9.6100c, 7.8400c, 7.8400c, 5.7600c, 1.2250d, 1.0240d, 3.6100c, 7.8400c, 1.0240d, 8.4100c, 8.4100c, 6.2500c, 4.0000c, 7.8400c, 2.2500c, 7.8400c, 6.2500c, 2.5600c, 4.0000c

Table 8: Outputs of dynamical quantum search algorithm for some probabilities of marked states $\rho_{r_1 r_2 r_3 r_4 r_5}$ ($r_1, r_2, r_3, r_4, r_5 = e, g$) and unmarked states of 5-qubit for different values of time, where $\frac{\gamma_1}{\lambda} = \frac{\theta_5}{113}$, $\frac{\gamma_2}{\lambda} = \frac{\theta_5}{90}$, $\frac{\gamma_3}{\lambda} = \frac{\theta_5}{140}$, $\frac{\gamma_4}{\lambda} = \frac{\theta_5}{100}$ and $\frac{\gamma_5}{\lambda} = \frac{\theta_5}{125}$; $a = \times 10^{-8}$ and $b = \times 10^{-7}$.

Times	$t = \frac{0.331\pi\hbar}{64\lambda\theta_6}$	$t = \frac{0.566\pi\hbar}{64\lambda\theta_6}$	$t_{6P} = \frac{0.9899\pi\hbar}{64\lambda\theta_6}$	$t = \frac{\pi\hbar}{64\lambda\theta_6}$
$\rho_{e e e e e e}$	0.3216	0.6082	0.7566	0.7566
$\rho_{e e e e g g}$	0.3365	0.6362	0.7914	0.7914
$\rho_{e e e g g e}$	0.3381	0.6389	0.7949	0.7950
$\rho_{e e g e e g}$	0.3357	0.6346	0.7895	0.7894
$\rho_{e e g g e e}$	0.3372	0.6374	0.7931	0.7930
$\rho_{e e g g g g}$	0.3531	0.6670	0.8299	0.8299
$\rho_{g e e e e g}$	0.3394	0.6416	0.7982	0.7982
$\rho_{g e e e g g}$	0.3471	0.6559	0.8162	0.8161
$\rho_{g e e g g e}$	0.3487	0.6588	0.8198	0.8197
$\rho_{g e g e e g}$	0.3463	0.6544	0.8141	0.8141
$\rho_{g e g g e e}$	0.3479	0.6573	0.8177	0.8178
$\rho_{g e g g g g}$	0.3643	0.6879	0.8561	0.8562
$\rho_{g e e e g e}$	0.3370	0.6369	0.7923	0.7923
$\rho_{g e e g e g}$	0.3469	0.6555	0.8155	0.8154
$\rho_{g e e g g g}$	0.3548	0.6702	0.8339	0.8339
$\rho_{g e g e g g}$	0.3519	0.6648	0.8272	0.8272
$\rho_{g e g g e g}$	0.3539	0.6685	0.8318	0.8319
$\rho_{g e g g g g}$	0.3619	0.6836	0.8506	0.8506
$\rho_{g g e e e g}$	0.3480	0.6575	0.8181	0.8179
$\rho_{g g e e g g}$	0.3579	0.6760	0.8412	0.8411
$\rho_{g g e g g g}$	0.3661	0.6912	0.8601	0.8603
$\rho_{g g g e e e}$	0.3545	0.6699	0.8335	0.8336
$\rho_{g g g e g g}$	0.3652	0.6896	0.8582	0.8582
$\rho_{g g g g g g}$	0.3736	0.7051	0.8777	0.8776

Table 10: Outputs of dynamical quantum search algorithm for some probabilities of marked states $\rho_{r_1 r_2 r_3 r_4 r_5 r_6}$ ($r_1, r_2, r_3, r_4, r_5, r_6 = e, g$) of 6-qubit for different values of time, where $\frac{\gamma_1}{\lambda} = \frac{\theta_6}{113}$, $\frac{\gamma_2}{\lambda} = \frac{\theta_6}{90}$, $\frac{\gamma_3}{\lambda} = \frac{\theta_6}{140}$, $\frac{\gamma_4}{\lambda} = \frac{\theta_6}{100}$, $\frac{\gamma_5}{\lambda} = \frac{\theta_6}{125}$ and $\frac{\gamma_6}{\lambda} = \frac{\theta_6}{119}$.

higher probabilities than any marked state probabilities through other times. Further increasing of γ_i and for different values of times, one can not distinguish the probabilities of some marked states for the different number of qubits, where some of un-marked states due to the influence of large dissipation exchange their values either increase or decrease the probabilities of marked states. Moreover, if dissipation rates are taken to be $\gamma_i = \lambda\theta_N$, $i = 1, 2, \dots, N$, one determines and observes at different times the probabilities of some marked states for different values of the number of N . However, when $\gamma_i > \lambda\theta_N$, we can not distinguish any marked states where very small values for the probability of marked state is shown. Which means that both marked and un-marked states have the same chance to contribute. One concludes that at $\gamma_i > \lambda\theta_N$, the system is destroyed completely as well as it can not search for any desired state whatever the number of qubits. It is interesting to discuss the influence of large values of dissipation on the probabilities of marked states at these optional times in the following scenario:

Through the optional times $\frac{0.331\pi\hbar}{2^N\lambda\theta_N}$ and the number of qubits up to $N = 5$, we can not distinguish and observe the probability of any marked state for any number of qubits except the probabilities of marked states of the kind $q_2 = \{gg, eg, ge\}$, $q_3 = \{ggg, egg, geg, gge\}$, $q_4 = \{gggg, eegg, gegg, ggge\}$ and $q_5 = \{ggggg, egggg, geggg, gggeg, gggeg, gggge\}$. As for the case of $N \geq 6$, we can not distinguish the probabilities of any marked states, where the probabilities of un-marked states show larger values compared with the probability of marked state which shows a small values.

At times $\frac{0.566\pi\hbar}{2^N\lambda\theta_N}$, one distinguishes the probability of marked state for 2-, 3- and 4-qubit but for 5-qubit one can not distinguish the probabilities of any marked states except the marked states which are of the kind q_5 one can distinguish the probabilities for it. While through this time when $N \geq 6$, we can not distinguish and determine the probability of any marked state, where both marked and un-marked states have the same chance to contribute in the search.

Also, at times t_{Np} , we distinguish the probability of any marked state for different number of qubits until $N = 5$ except the probabilities of the marked states $|eeee\rangle$ and $|eeeee\rangle$. For $N = 6$, one can not observe and determine the probability of any marked state except the marked states of the kind $q_6 = \{gggggg, eggggg, gegggg, ggeggg, gggegg, ggggeg, ggggge\}$, where the value of any marked state probability for this kind is distinguished and shows small value and larger than the probabilities of the remaining states. However, we expect through these times for $N > 6$ that one can not distinguish and determine the probability of any marked state.

Finally, at times $\frac{\pi\hbar}{2^N\lambda\theta_N}$, it is shown that the probability of any marked state for the different number of qubits until $N = 4$ can be distinguished. As for 5-qubit and 6-qubit, we can not distinguish the probability of some marked state, see Tables (9,11), except the marked states of the kind q_5 and q_6 . After that, through these times, one can not observe the probabilities of any marked states at $N = 7$ and more. Consequently, through the large dissipation values, most marked states are distinguished through the optional times t_{Np} for the different number of qubits. As a result, one can distinguish and observe, at large values of dissipation, the probabilities of many different marked states for multi qubits at different values of times. These observations give an advantage of using the dynamical quantum search algorithm with the dissipation are other quantum search algorithms.

References

- [1] L. K. Grover, A fast quantum mechanical algorithm for database search, in Proc., 28th Annual ACM Symposium on the Theory of Computing, New York, pp. 212 (1996).
- [2] L. K. Grover, Quantum mechanics helps in searching for a needle in a haystack, *Phys. Rev. Lett.*, **79**, 325 (1997).
- [3] L. DiCarlo, J. M. Chow, J. M. Gambetta, Lev S. Bishop, B. R. Johnson, D. I. Schuster, J. Majer, A. Blais, L. Frunzio, S. M. Girvin and R. J. Schoelkopf, Demonstration of two-qubit algorithms with a superconducting quantum processor, *Nature* **460**, 240 (2009).
- [4] W.-L. Yang, H. Wei, C.-Y. Chen and M. Feng, Implementation of a many-qubit Grover search with trapped ultracold ions, *J. Opt. Soc. Am. B* **25**, 1720 (2008).
- [5] Z. J. Deng, M. Feng and K. L. Gao, Simple scheme for the two-qubit Grover search in cavity QED, *Phys. Rev. A* **72**, 034306 (2005).
- [6] W. L. Yang, C. Y. Chen and M. Feng, Implementation of three-qubit Grover search in cavity quantum electrodynamics, *Phys. Rev. A* **76**, 054301 (2007).
- [7] I. L. Chuang, N. Gershenfeld and M. Kubinec, Experimental Implementation of Fast Quantum Searching, *Phys. Rev. Lett.* **80**, 3408 (1998).
- [8] L. K. Grover, Fixed-Point Quantum Search, *Phys. Rev. Lett.* **95**, 150501 (2005).
- [9] G. L. Long, Y. S. Li, W. L. Zhang and L. Niu, Phase matching in quantum searching, *Phys. Lett. A* **262**, 27 (1999).
- [10] M. H. S. Amin, Peter J. Love, and C. J. S. Truncik, Thermally Assisted Adiabatic Quantum Computation, *Phys. Rev. Lett.* **100**, 060503 (2008).
- [11] I. de Vega, M. Carmen Banuls and A Perez, Effects of dissipation on an adiabatic quantum search algorithm, *New J. Phys.* **12**, 123010 (2010).
- [12] M. Macovei, J. Evers, and C. H. Keitel, Quantum entanglement in dense multiqubit systems, *J. Mod. Opt.* **14 & 15**, 1287 (2010).
- [13] C. Chen, Z. Chen, J. Liang, Simulation of the superradiant quantum phase transition in the superconducting charge qubits inside a cavity, *Phys. Rev. A* **76**, 055803 (2007).
- [14] K. Xia, M. Macovei, J. Evers and C. H. Keitel, Robust coherent preparation of entangled states of two coupled flux qubits via dynamic control of the transition frequencies, *Phys. Rev. B* **79**, 024519 (2009).
- [15] Y. N. Chen, D. S. Chuu, T. Brandes, Current Detection of Superradiance and Induced Entanglement of Double Quantum Dot Excitons, *Phys. Rev. Lett.* **90**, 166802 (2003).
- [16] M. W. Johnson, M. H. S. Amin, S. Gildert, T. Lanting, F. Hamze, N. Dickson, R. Harris, A. J. Berkley, J. Johansson, P. Bunyk, E. M. Chapple, C. Enderud, J. P. Hilton, K. Karimi, E. Ladizinsky, N. Ladizinsky, T. Oh, I. Perminov, C. Rich, M. C. Thom, E. Tolkacheva, C. J. S. Truncik, S. Uchaikin, J. Wang, B. Wilson and G. Rose, "Quantum annealing with manufactured spins," *Nature* **473**, 194 (2011).

- [17] R. Harris, M. W. Johnson, T. Lanting, A. J. Berkley, J. Johansson, P. Bunyk, E. Tolkacheva, E. Ladizinsky, N. Ladizinsky, T. Oh, F. Cioata, I. Perminov, P. Spear, C. Enderud, C. Rich, S. Uchaikin, M. C. Thom, E. M. Chapple, J. Wang, B. Wilson, M. H. S. Amin, N. Dickson, K. Karimi, B. Macready, C. J. S. Truncik and G. Rose, Experimental investigation of an eight-qubit unit cell in a superconducting optimization processor, *Phys. Rev. B* **82**, 024511 (2010).